Shahahmadi, Ahmad; Kivisaari, Pyry; Behaghel, Benoît; Radevici, Ivan; Suihkonen, Sami; Oksanen, Jani

Pushing the limits of non-radiative recombination suppression in GaAs/GaInP light emitting diodes by doping profile engineering

Published in:
Applied Physics Letters

Published: 13/06/2024

Document Version
Peer-reviewed accepted author manuscript, also known as Final accepted manuscript or Post-print

Please cite the original version:
Shahahmadi, A., Kivisaari, P., Behaghel, B., Radevici, I., Suihkonen, S., & Oksanen, J. (2024). Pushing the limits of non-radiative recombination suppression in GaAs/GaInP light emitting diodes by doping profile engineering. *Applied Physics Letters*, *124*, 1-6. Article 241105.

-

Pushing the limits of non-radiative recombination suppression in GaAs/GaInP light emitting diodes by doping profile engineering

Seyed Ahmad Shahahmadi*,[1] Pyry Kivisaari,[1] Benoît Behaghel,[1] Ivan Radevici,[1] Sami Suihkonen,[1] and Jani Oksanen[1]
Engineered Nanosystems Group, Aalto University, Aalto 00076, Finland.
(*Electronic mail: ahmad.shahahmadi@aalto.fi)

(Dated: 31 May 2024)

Optimizing the efficiency of optoelectronic devices is challenging at low currents, even with high-quality materials, due to the dominance of non-radiative Shockley-Read-Hall recombination at low carrier densities. In this study, we nearly eliminate the typical non-radiative recombination current in a GaAs/GaInP double-heterojunction light emitting diode (LED) by shifting the *pn*-junction 200 nm into the GaInP barrier layer on the *n*-side. This involves reducing the doping in the *n*-barrier to below the background *p*-type doping level to relocate the built-in electric field. As a result, the space charge recombination current with the ideality factor of two is strongly suppressed and remains concealed in our experimental dark current density-voltage measurements. The experimental results, coupled with our physics-based model, indicate the potential for considerable efficiency gains at current densities below $\sim$1 A/cm^2. The findings prompt to carefully optimize the doping profiles of high efficiency LEDs and to reconsider the validity of using dark saturation currents as a metric for their performance.

In optoelectronics, crystal imperfections within bulk layers and interfaces serve as sites for non-radiative recombination through the Shockley-Read-Hall (SRH) recombination process[1]. The minimization of SRH recombination is particularly essential to improve the internal quantum efficiency (IQE) in light-emitting diodes (LEDs) often referred as the internal radiative efficiency in photovoltaic (PV) cells, necessary for optimizing their performance[2,3]. In both device types, the SRH recombination typically dominates the low voltage part of the dark current, exhibiting an ideality factor (n_{id}) of two[4]. Consequently, optoelectronic device efficiency at low current densities is generally considered to be low, even in devices of high material quality. This picture is based on the assumption that the depletion region is located in the active region of LEDs (or the absorber in the case of PV cells).

Within the domain of III-V PVs, it has been established that SRH recombination can be strongly reduced by adopting suitable heterojunction structures, such as the *n*-GaInP/*p*-GaAs structure, where the emitter layer is made of a wider band gap material, instead of using customary GaAs *pn*-homojunctions[5,6]. This reference point was also recently employed to demonstrate the concept that partly shifting the depletion region to the wider band gap barrier layers can be beneficial in GaInAsP LEDs emitting at 0.9 eV[7]. In this pioneering study, the doping was switched from *n* to *p* at the GaInAsP/InP heterointerface with dopant densities pushing most of the depletion layer into the InP barrier. The theoretical considerations suggested a major reduction in the SRH recombination rate. As the experimental result, SRH recombination was estimated to decrease to $\sim$25% of its value in the control LED with a conventional doping profile. This improvement also enabled an increase in the IQE at lower current densities when compared to the control sample.

Achieving high LED IQE, even at low currents ($\leq$ 1 A/cm^2), is particularly necessary for emerging applications such as the electroluminescent cooling (ELC)[8] and the closely related thermophotonic energy harvesting applications[9,10]. In GaAs-based LEDs, where peak IQEs can be expected to match the high IQEs reported for photoluminescence surpassing 99%[11–13], being able to extend the regime of peak efficiency holds significant importance. Additional applications could also be found for LEDs in radio frequency and optical wireless communication, where high efficiencies at low currents are beneficial[14,15]. Thus, the identification of pathways to stretch the high IQE regime of LEDs towards lower currents holds profound implications for the evolution of emerging LED technologies.

In this study, we suppress the $n_{id} = 2$ current of the GaAs/GaInP double heterojunction (DHJ) LED by several orders of magnitude through a redesign of the doping profile, pushing the *pn*-junction further into the *n*-side barrier region instead of locating it at the interface between the active region and the barrier as in the previous works. This design shares apparent similarities with so-called diffusion-driven LEDs[16,17]. However, here the structure remains essentially 1D, and the purpose is to suppress SRH recombination instead of enabling near-surface light emitters or large-area devices. The suppression is demonstrated through a combination of secondary ion mass spectrometry (SIMS) and dark current density-voltage measurements. The observed outcomes are further elucidated through comprehensive full-device simulations and the fundamental models of SRH recombination.

Two GaAs/GaInP DHJ LEDs were compared in this study, grown epitaxially using metalorganic vapor-phase epitaxy (MOVPE). Fig. 1 illustrates the schematics of our control reference LED (Ctrl-LED) and the shifted junction LED (Shft-LED). Detailed information about the GaAs/GaInP DHJ configurations is provided in Table I. The Ctrl-LED is a typical DHJ LED with an unintentionally doped GaAs active region, while the Shft-LED is a sample where the position of the *pn*-junction has been deliberately shifted into the *n*-type GaInP barrier. For both samples, we used a constant growth temperature of 595°C (wafer surface temperature), with V/III ratios maintained at approximately 11, 26, and 66 for GaAs, AlGaAs, and GaInP, respectively. The doping sources included diethylzinc for *p*-type doping and disilane for *n*-type doping, both utilized during the growth process. The background doping within the reactor was *p*-type, measuring at 1×10^{16} cm^{-3} or slightly less for GaAs according to Hall setup measurements. Furthermore, SIMS measurements gave an unintentional C doping of $\sim 2 \times 10^{16}$ cm^{-3} for unintentionally doped GaInP, and confirmed that in GaAs it is $\leq 1 \times 10^{16}$ cm^{-3}. This *p*-type doping can be attributed to the unintentional inclusion of C byproducts from III-V materials during the growth process. The C may serve as a *p*-type dopant by substituting for an As site[18].

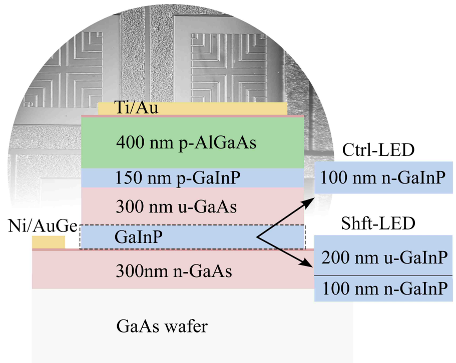

FIG. 1. Cross-section of the investigated double heterojunction GaAs LEDs, emphasizing the distinctions in layer structure between the Ctrl and Shft-LEDs. The background image displays the physical device under an optical microscope, with LEDs 1 mm^2 in mesa size. Samples chosen for the present study were covered by a full p-contact.

After growth, the LEDs underwent simultaneous processing, involving ultraviolet lithography and selective wet etching to define 1 mm x 1 mm mesas. Electron beam evaporation was used to establish the electrical contacts, Ti/Au was deposited as the p-type contact, and subsequently, n-contacts were formed using Ni/AuGe, followed by rapid thermal annealing at 350°C for 15 seconds.

TABLE I. Design carrier concentration of the fabricated double hetero-junction GaInP/GaAs/GaInP LEDs, also corresponding to the concentrations obtained from the Hall measurements (in units of /cm^3) of standalone reference layers. The choice of 200 nm as the thickness of the u-GaInP layer in Shft-LED is discussed in the analysis.

Device	p-GaInP 50 nm	p-GaInP 100 nm	u-GaAs 300 nm	u-GaInP 200 nm	n-GaInP 100 nm
Ctrl-LED	1×10^{18}	4×10^{17}	1×10^{16}	-	-2×10^{17}
Shft-LED	1×10^{18}	4×10^{17}	1×10^{16}	2×10^{16}	-2×10^{17}

Later, the electrical characteristics of the LEDs were assessed using a four-probe arrangement in combination with a Keithley source meter unit. The most conventional signature for non-radiative recombination in LEDs is the specific exponential dependence of current density (J) on its bias voltage (V). More quantitatively, the $J(V)$ curve often exhibits clear regimes that follow the Shockley diode equation $J_{0,n_{id}}\left(e^{U/n_{id}V_T}-1\right)$, where the n_{id} adopts a value of 1 or 2. In the regime with the $n_{id}=2$, the J_{02} is usually considered to reflect the magnitude of SRH recombination in the depletion region. The corresponding dark saturation current J_{02} for a high-quality device is considered to be of the order of 1×10^{-12} A/cm^2 in both GaAs-based LEDs and PVs, and major efforts in growth, passivation, and processing optimization have been directed towards reducing the dark saturation currents arising both from the SRH recombination in the depletion layer, as well as from the surface recombination on the mesa perimeter[4,17,19–23]. However, if the electrostatics and carrier dynamics of the device are engineered e.g. by modifying the doping profile as done in this study, it becomes possible for the low voltage operation of the optoelectronic device to no longer be dominated by the $n_{id}=2$ current. This experimental finding has implications both for the characterization of SRH recombination and for the optimization of optoelectronic devices.

The effect of shifting the junction on the $J(V)$ curve was further analyzed through standard full-device simulations, accounting for drift and diffusion currents, self-consistent electric fields, as well as carrier density-dependent SRH, radiative and Auger recombination rates similarly as in our previous works[24]. The most fundamental element in the simulations explaining the mechanisms for reduced SRH recombination due to shifting the depletion region is directly captured in the well-known SRH recombination law that can be written in the customary single trap level form as[1]:

$$R_{srh}=\frac{np-n_i^2}{\tau_p(n+n_i)+\tau_n(p+n_i)}, \tag{1}$$

where τ_n and τ_p are the SRH lifetimes for electrons and holes, n and p are the electron and hole densities, respectively, and n_i is the intrinsic carrier density. n_i in the denominator follows from assuming that the dominant trap level is located roughly in the middle of the band gap. This single trap level form typically allows reproducing the experimental behavior of LEDs, but studying the trap spectrum more thoroughly could provide additional insight. Nevertheless, this equation accounts for the changes in the n_{id} and magnitude of SRH recombination and is referred to later when analyzing the results of the paper. In the simulations, we use $\tau_p=\tau_n=6.25\times10^{-8}$ s and a radiative recombination coefficient of 7.2×10^{-10} cm^3/s[25]. The simulations are carried out in 1D (=effectively assuming an infinite structure in the two remaining dimensions), and the contacts are described by the customary Dirichlet boundary conditions specifying the applied bias of the LED.

Fig. 2 shows the atomic concentrations of C and Si in the GaAs active layer and the n-side of the GaInP barrier layer below the active layer as analyzed by SIMS in the Ctrl-LED (a) and the Shft-LED (b). The results indicate that the C background concentration in GaAs remains at or below the detection limit of 1×10^{16} at/cm^3 in both devices, while the GaInP layers exhibit a slightly higher C concentration at $\sim2\times10^{16}$ at/cm^3. Regarding the concentration of Si atoms, it remains approximately constant at 2×10^{17} at/cm^3 over a 100 nm GaInP barrier layer in the Ctrl-LED, however the doping profile in the 300 nm thick GaInP barrier in the Shft-LED is completely different. In the Shft-LED, the Si atom levels first stay below the background doping levels in the GaInP barrier next to the active region, making C the dominant contributor to the dopant profile in the first 200 nm of the barrier. After this the Si atom density increases gradually from 2×10^{15} to 2×10^{17} at/cm^3. The initial values presented in Table I align with the Hall and SIMS measurements, and these values are also used in the simulations. Most importantly, the C doping in the u-GaInP layer is 2×10^{16} cm^{-3}, shifting the pn junction into the n-side. For u-GaAs, we assume the C doping to be at the identified upper limit of 1×10^{16} cm^{-3} (to be shortly commented on in the analysis).

Fig. 3(a) shows the measured $J(V)$ curves of the Ctrl-LED and Shft-LED, along with ideal diode curves corresponding to $n_{id}=1$ and $n_{id}=2$ for additional insight. The $J(V)$ curve of Ctrl-LED primarily constitutes of an $n_{id}=2$ nonradiative SRH current with a fitted J_{02} prefactor of 6.2×10^{-11} A/cm^2. On the other hand, the $J(V)$

curve of Shft-LED does not exhibit a clear n_{id} = 2 component within the measured voltage range. The fact that no $n_{id} = 2$ behaviour can be seen at this voltage range effectively sets an upper bound for the J_{02} value of Shft-LED at around 3×10^{-13} A/cm^2. This is over 2 orders of magnitude smaller than the J_{02} estimated for Ctrl-LED, and therefore provides an experimental verification of the major SRH reduction potential anticipated also in Ref[7]. This major difference between Ctrl-LED and Shft-LED is caused by differences in how the depletion region is located in the two devices, as explained in more detail in the following paragraphs with the help of simulations. The experimental curves can be compared with the simulated ones shown in Fig. 3(b). There, one can observe that the $J(V)$ curves simulated for Ctrl-LED and Shft-LED well match the trends of their experimental counterparts, most importantly with Shft-LED exhibiting no visible J_{02} current component (see caption of Fig. 3 for discussion on the slight differences). Preliminary light emission measurements are provided in the Supplementary material, indicating essentially no difference in the radiative current as a function of bias between the two samples.

Simulations and the underlying theory allow studying the reasons behind the suppressed nonradiative $n_{id} = 2$ current in the Shft-LED sample. The largest contributions to the SRH current with $n_{id} = 2$ arises when electron and hole concentrations are equal ($n = p$) and exponentially depend on the voltage. Therefore, the SRH recombination with $n_{id} = 2$ can be seen as a signature of SRH recombination within the depletion region. If $n = p$ is located in the material that has the highest n_i within the device, SRH recombination also reaches its maximum there (assuming no orders-of-magnitude spatial changes in τ_n and τ_p). Figure 4(a) shows the simulated SRH recombination rate along with the electron and hole densities in the Ctrl-LED sample at an applied bias of 0.8 V. There, the condition $n = p$ is reached in the GaAs active layer roughly at the depth of 0.77 μm from the device surface. The SRH recombination curve in the figure reaches its maximum value at a point where $n = p$ and clearly dominates over the radiative recombination at this bias. Its dependence on the voltage exhibits the $n_{id} = 2$ in the simulations, in line with the well-known SRH recombination theory of Eq. (1).

The SRH recombination rate simulated for the Shft-LED sample is shown in Fig. 4(b), again together with the electron and hole densities and at the applied bias of 0.8 V. In Fig. 4(b), the electron and hole densities cross only in the GaInP layer to the right from the active region. Therefore one can observe that the depletion region has been

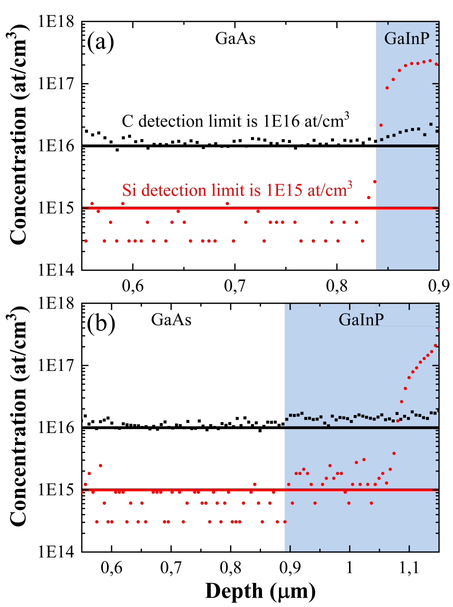

FIG. 2. Secondary ion mass spectrometry profiles of C and Si in undoped-GaAs/n-GaInP interface for (a) Ctrl-LED, and (b) Shft-LED. The GaInP barrier layer is marked with a blue background.

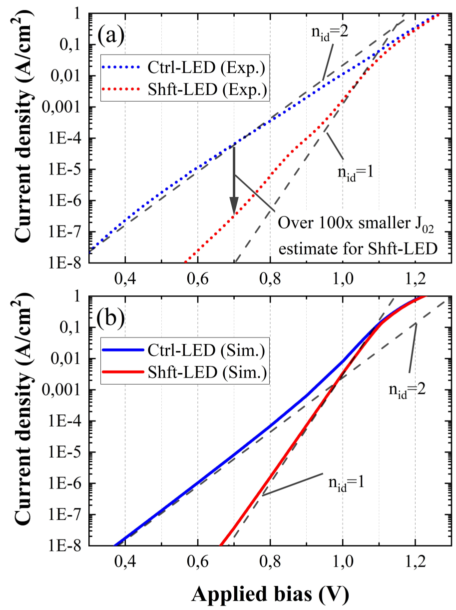

FIG. 3. (a) Measured current density-voltage $J(V)$ curves for the Ctrl-LED and Shft-LED samples, along with the curves corresponding to ideality factors 2 and 1 added for visual guidance. (b) $J(V)$ curves for the Ctrl-LED and Shft-LED from drift-diffusion simulations, also with the guiding $n_{id} = 1$ and $n_{id} = 2$ curves. Both simulated curves in (b) include an additional series resistivity of 5×10^{-2} Ωcm^2 to account for an effective contact and current spreading resistance phenomenologically describing charge spreading resistance in the 1 mm^2 large samples, and for possible other nonidealities. This value is chosen to provide a qualitative agreement with the experimental curves between 1.0–1.2 V. The slight differences between the experimental and simulated $J(V)$ curves of the Shft-LED sample at the small biases are expected to be due to additional surface and/or interface recombination currents that were not considered in the simulations. Note also that without the suppression of the $n_{id} = 2$ current such processes would remain hidden by the large SRH induced component of the current. Regarding the data in (b), the $qU - \Delta E_F$ value (ΔE_F being the average quasi-Fermi level separation in the GaAs active layer) differs by roughly 0.01 $k_B T$ or less between the two samples at all voltages.

shifted towards the n-side, explaining also the name of the sample. The SRH recombination rate in GaInP is much larger in Shft-LED [Fig. 4(b)] than in Ctrl-LED [Fig. 4(a)] and it exhibits the $n_{id} = 2$ in the simulations. However, due to the orders-of-magnitude smaller n_i of GaInP, the dominant SRH recombination is still the one taking place in the GaAs. There, throughout the GaAs active layer in Fig. 4(b), the hole density is several orders of magnitude larger than electron density thanks to both (*i*) the n-type doping starting only relatively far from the GaAs active layer and (*ii*) the presence of a light p-type background doping density in GaAs and the GaInP layer next to it. In such a case, the SRH recombination rate from Eq. (1) produces the $n_{id} = 1$ behavior, with the corresponding SRH recombination rate in GaAs in Shft-LED [Fig. 4(b)] being considerably smaller than in Ctrl-LED [Fig. 4(a)].

Moreover, Fig. 4 illustrates the simulated radiative recombination rate. Since the quasi-Fermi level splitting in the GaAs active layer (not shown) is practically constant in the active region and equal to the applied bias for both samples, the radiative recombination rate is practically identical between Fig. 4(a) and (b), despite the distinct electron-hole profiles (constant quasi-Fermi level splitting ensures that np is constant even if n and p vary due to band bending; radiative recombination follows $B(np - n_i^2)$, where B is the recombination coefficient). As previously explained, the n_{id} of the dominating SRH recombination current is likewise equal to 1 in the Shft-LED. Consequently, even the total $J(V)$ curve of the Shft-LED exhibits the $n_{id} = 1$ in Fig. 3(b) within this voltage range, with minor J_{02} current component (the slight deviation from $n_{id} = 1$ is attributed to minor SRH recombination in GaInP, as discussed earlier). Here, the thickness of the u-GaInP layer in Shft-LED (see Table I) is an important parameter: it should be large enough to push the $n_{id} = 2$ SRH current to the GaInP barrier but not too large to cause additional quasi-Fermi level losses (this is also a design challenge that Shft-LED shares with diffusion-driven LEDs). Based on the results of this paper, a thickness of 200 nm fulfills these requirements. Furthermore, the light emission measurements provided in the Supplementary material accentuate that the shifted junction does not hamper current transport to the GaAs active layer and thereby reduce its radiative current. Therefore the reduced total current of Shft-LED can be interpreted namely as a signature of suppressed non-radiative recombination.

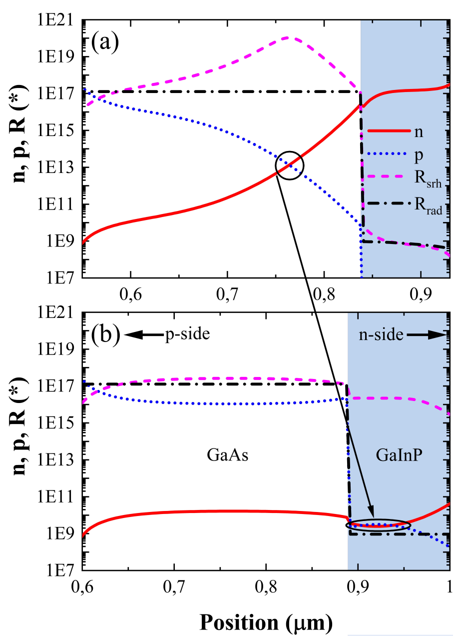

FIG. 4. Electron density n, hole density p, SRH recombination rate R_{srh}, and radiative recombination rate R_{rad} as a function of position for (a) Ctrl-LED and (b) Shft-LED, simulated at an applied bias (= voltage between the LED contact terminals) of 0.8 V. The GaInP barrier layer is marked with a blue background. Differences between the Ctrl-LED and Shft-LED samples illustrated in this figure explain the vastly different $J(V)$ curves of the two devices shown in Fig. 3. The $qU - \Delta E_F$ value (see caption of Fig. 3) is less than 10^{-3} k_BT in both samples at this voltage.
* Units: (cm^{-3}) for n and p, and ($cm^{-3}s^{-1}$) for R_{srh} and R_{rad}.

In the Shft-LED sample studied in Fig. 4(b), the maximum value of SRH recombination is indeed more than two orders of magnitude smaller than in Ctrl-LED in Fig. 4(a) despite the same SRH recombination coefficients, while radiative recombination in GaAs is equal in Fig. 4(a) and (b). The IQE of the Shft-LED sample is therefore expected to be notably higher than that of Ctrl-LED and roughly constant at the corresponding low-to-medium current levels. Consequently, the eventual IQE within the current range still depends on the material quality (due to both SRH and radiative currents having $n_{id} = 1$, $n_{id} = 1$ does not automatically mean that radiative recombination dominates). This underscores the importance of maintaining high epitaxial and processing quality, even in samples with a shifted junction. Additionally, the IQE may depend on a more refined engineering of the doping profile in the shifted junction, where the exact C doping level in GaAs could also play a role. However, the investigation of these dependencies is beyond the scope of this work.

In conclusion, we have demonstrated that shifting the pn-junction of the GaInP/GaAs DHJ LED from the edge of the active region to 200 nm into the originally n-type doped GaInP barrier layer practically eliminates conventionally dominant non-radiative SRH recombination in the devices, while radiative recombination remains uncompromised. This alteration dramatically impacts the $J(V)$ characteristics of the device, leading to the disappearance of the typical SRH-dominated current regime exhibiting the $n_{id} = 2$ at low currents. This shift potentially uncovers previously obscured features in the $J(V)$ normally hidden under the strong SRH-dominated components. The findings indicate that using dark saturation currents of $n_{id} = 2$ as a metric for device quality may be insufficient when applied to devices with unconventional doping profiles. However, the findings can also help to extend the operating regime where LEDs or solar cells exhibit their peak quantum efficiencies. This extension would significantly facilitate the development of high-efficiency devices, especially for photovoltaic and thermophotonic applications.

Please refer to the Supplementary material for details on the preliminary light emission measurements conducted for the Ctrl-LED and Shft-LED samples discussed in this study.

We acknowledge financial support from the European Union's Horizon 2020 programme (Grant Agreement Nos. 951976 and 964698) and the Research Council of Finland (13343312). We also wish to thank the provision of facilities and technical support by Aalto University at OtaNano-Micronova Nanofabrication Centre and the Aalto Science-IT project.

[1] W. Shockley and W. T. Read. Statistics of the recombinations of holes and electrons. *Phys. Rev.*, 87:835–842, Sep 1952.

[2] John F. Geisz, Myles A. Steiner, Iván García, Ryan M. France, Daniel J. Friedman, and Sarah R. Kurtz. Implications of redesigned, high-radiative-efficiency GaInP junctions on III-V multijunction concentrator solar cells. *IEEE Journal of Photovoltaics*, 5(1):418–424, 2015.

[3] P. Espinet-González, I. Rey-Stolle, M. Ochoa, C. Algora, I. García, and E. Barrigón. Analysis of perimeter recombination in the subcells of GaInP/GaAs/Ge triple-junction solar cells. *Progress in Photovoltaics: Research and Applications*, 23(7):874–882, 2015.

[4] Luc M. van der Krabben, Natasha Gruginskie, Maarten van Eerden, Jasper van Gastel, Peter Mulder, Gerard J. Bauhuis, Dinar Khusyainov, Dima Afanasiev, Elias Vlieg, and John J. Schermer. Reduced surface recombination in extended-perimeter LEDs toward electroluminescent cooling. *ACS Applied Electronic Materials*, 0(0):null, 0.

[5] Tetsuya Nakamura, Warakorn Yanwachirakul, Mitsuru Imaizumi, Masakazu Sugiyama, Hidefumi Akiyama, and Yoshitaka Okada. Reducing Shockley–Read–Hall recombination losses in the depletion region of a solar cell by using a wide-gap emitter layer. *Journal of Applied Physics*, 130(15):153102, 10 2021.

[6] Kevin L. Schulte, John Simon, Myles A. Steiner, and Aaron J. Ptak. Modeling and design of III-V heterojunction solar cells for enhanced performance. *Cell Reports Physical Science*, 4(9):101541, 2023.

[7] Parthiban Santhanam, Wei Li, Bo Zhao, Chris Rogers, Jr. Gray, Dodd Joseph, Phillip Jahelka, Harry A. Atwater, and Shanhui Fan. Controlling the dopant profile for SRH suppression at low current densities in $\lambda \approx 1330$ nm GaInAsP light-emitting diodes. *Applied Physics Letters*, 116(20):203503, 05 2020.

[8] Toufik Sadi, Ivan Radevici, and Jani Oksanen. Thermophotonic cooling with light-emitting diodes. *Nature Photonics*, 14(4):205–214, 2020.

[9] Julien Legendre and Pierre-Olivier Chapuis. GaAs-based near-field thermophotonic devices: Approaching the idealized case with one-dimensional pn junctions. *Solar Energy Materials and Solar Cells*, 238:111594, 2022.

[10] Ivan Radevici, Jonna Tiira, Toufik Sadi, Sanna Ranta, Antti Tukiainen, Mircea Guina, and Jani Oksanen. Thermophotonic cooling in GaAs based light emitters. *Applied Physics Letters*, 114(5):051101, 02 2019.

[11] H. Gauck, T. H. Gfroerer, M. J. Renn, E. A. Cornell, and K. A. Bertness. External radiative quantum efficiency of 96% from a GaAs/GaInP heterostructure. *Applied Physics A*, 64(2):143–147, 1997.

[12] I. Schnitzer, E. Yablonovitch, C. Caneau, and T. J. Gmitter. Ultrahigh spontaneous emission quantum efficiency, 99.7 *Applied Physics Letters*, 62(2):131–133, 01 1993.

[13] Nathan Giannini, Zhou Yang, Ashish K. Rai, Alexander R. Albrecht, and Mansoor Sheik-Bahae. Near-unity external quantum efficiency in GaAs|AlGaAs heterostructures grown by molecular beam epitaxy. *physica status solidi (RRL) – Rapid Research Letters*, 15(6):2100106, 2021.

[14] Jaehee Cho, E. Fred Schubert, and Jong Kyu Kim. Efficiency droop in light-emitting diodes: Challenges and countermeasures. *Laser & Photonics Reviews*, 7(3):408–421, 2013.

[15] Ning Li, Kevin Han, William Spratt, Stephen Bedell, John Ott, Marinus Hopstaken, Frank Libsch, Qinglong Li, and Devendra Sadana. Ultra-low-power sub-photon-voltage high-efficiency light-emitting diodes. *Nature Photonics*, 13(9):588–592, 2019.

[16] Lauri Riuttanen, Pyry Kivisaari, Olli Svensk, Jani Oksanen, and Sami Suihkonen. Electrical injection to contactless near-surface InGaN quantum well. *Appl. Phys. Lett.*, 107:051106, Aug 2015.

[17] Antti Myllynen, Seyed Ahmad Shahahmadi, Ivan Radevici, and Jani Oksanen. Back-contacted GaInP/GaAs LED structures by ex-situ dopant redistribution. *IEEE Transactions on Electron Devices*, 70(10):5156–5162, 2023.

[18] Giacomo Giorgi, Michele Amato, Stefano Ossicini, Xavier Cartoixà, Enric Canadell, and Riccardo Rurali. Doping of III–V arsenide and phosphide wurtzite semiconductors. *The Journal of Physical Chemistry C*, 124(49):27203–27212, 2020.

[19] Nicklas Anttu, Vilgail ė Dagytė, Benoît Behaghel, Ivan Radevici, Toufik Sadi, Pyry Kivisaari, and Jani Oksanen. Electro-optical coupling in double diode structures. *Phys. Rev. Appl.*, 19:064054, Jun 2023.

[20] T. Patrick Xiao, Kaifeng Chen, Parthiban Santhanam, Shanhui Fan, and Eli Yablonovitch. Electroluminescent refrigeration by ultra-efficient GaAs light-emitting diodes. *Journal of Applied Physics*, 123(17):173104, 05 2018.

[21] Natasha Gruginskie, Federica Cappelluti, Maarten van Eerden, Gerard Bauhuis, Peter Mulder, Elias Vlieg, and John Schermer. Proton irradiation induced gaas solar cell performance degradation simulations using a physics-based model. *Solar Energy Materials and Solar Cells*, 223:110971, 2021.

[22] Tripurari S. Tripathi, Ivan Radevici, Vilgailė Dagytė, Toufik Sadi, and Jani Oksanen. Improving the efficiency of GaInP/GaAs light emitters using surface passivation. *IEEE Transactions on Electron Devices*, 67(9):3667–3672, 2020.

[23] Brendan M. Kayes, Hui Nie, Rose Twist, Sylvia G. Spruytte, Frank Reinhardt, Isik C. Kizilyalli, and Gregg S. Higashi. 27.6% conversion efficiency, a new record for single-junction solar cells under 1 sun illumination. In *2011 37th IEEE Photovoltaic Specialists Conference*, pages 000004–000008, 2011.

[24] Toufik Sadi, Ivan Radevici, Pyry Kivisaari, and Jani Oksanen. Electroluminescent cooling in III–V intracavity diodes: Efficiency bottlenecks. *IEEE Transactions on Electron Devices*, 66(6):2651–2656, 2019.

[25] M. Levinshtein, S. Rumyantsev, and M. Shur. *Handbook Series on Semiconductor Parameters. Volume 1: Si, Ge, C (Diamond), GaAs, GaP, GaSb, InAs, InP, InSb*. World Scientific, Singapore, 1996.